



Contents lists available at ScienceDirect

Journal of Sound and Vibration

journal homepage: www.elsevier.com/locate/jsvi

Sweep excitation with order tracking: A new tactic for beam crack analysis

Dongdong Wei ^a, KeSheng Wang ^{a,*}, Mian Zhang ^a, Ming J. Zuo ^{a,b}

^a School of Mechatronics Engineering, University of Electronic Science and Technology of China, Equipment Reliability, Prognostics and Health Management Lab (ERPHM), China

^b Department of Mechanical Engineering, University of Alberta, Edmonton, Alberta, T6G 2G8, Canada

ARTICLE INFO

Article history:

Received 5 July 2017

Revised 20 November 2017

Accepted 9 January 2018

Available online 3 February 2018

Keywords:

Beam crack analysis

Sweep excitation

Order tracking

ABSTRACT

Crack detection in beams and beam-like structures is an important issue in industry and has attracted numerous investigations. A local crack leads to global system dynamics changes and produce non-linear vibration responses. Many researchers have studied these non-linearities for beam crack diagnosis. However, most reported methods are based on impact excitation and constant frequency excitation. Few studies have focused on crack detection through external sweep excitation which unleashes abundant dynamic characteristics of the system. Together with a signal resampling technique inspired by Computed Order Tracking, this paper utilize vibration responses under sweep excitations to diagnose crack status of beams. A data driven method for crack depth evaluation is proposed and window based harmonics extracting approaches are studied. The effectiveness of sweep excitation and the proposed method is experimentally validated.

© 2018 Elsevier Ltd. All rights reserved.

1. Introduction

Condition monitoring and maintenance planning of beam and beam-like structures are critical in various industrial applications, such as civil engineering, aerospace and automotive. Detection and evaluation of beam cracks caused by mechanical fatigue and chemical corrosion become important issues for structural health monitoring and maintenance [1]. Among various monitoring techniques, vibration monitoring has been reported to be both practical and effective for many fault diagnostic problems including beam crack evaluation [2–4].

Vibration based monitoring may be classified into model based and data driven categories. Model based methods construct mathematical models to study the dynamic behaviour of the beam under different crack status [5,6], while data driven methods use historical data to match vibration patterns [7–9]. Both two approaches involve extracting effective features, such as natural frequencies and harmonics, from vibrational signals.

Early researchers developed many ways for beam modelling. Dimarogonas [10] (1996) and Bovsunovsky and Surace [11] (2015) surveyed beam models for crack detection. In Refs. [12–14], the cracks are assumed to be open. Many other works, e.g. Refs. [15–18], took the closing effect into account and established breathing crack models. It is found that the stiffness changes as the two bodies of the beam on either hand of the crack come into contact and depart. Beam models with breathing crack are reported to be more sensitive to small cracks [19] and exhibit non-linear characteristics of the system. The non-linearity caused by breathing phenomenon are often been studied as a key to crack analysis in beams. Some diagnostic methods monitor the non-linear changes of modal shapes [20,21] or natural frequencies [5,22,23] to determine crack status. However, Loutridis et al.

* Corresponding author.

E-mail address: keshengwang@uestc.edu.cn (K. Wang).

[24] and Kim and Stubbs [25] pointed out that these changes are fractional to crack conditions. Instead, many papers, such as [26,27], use non-linear characteristics of the response to diagnose the beams. Sub and super harmonics are typical non-linear features that are used to indicate crack status of the beam [17,28]. In Section 2.1, an analytical demonstration is given in order to explain the relationship between crack status and the harmonics in its vibration response.

To vibrate the beam, most reported researches use impact force (hammer test) [29,30] or sinusoidal force (harmonic excitation) [31–33]. Hammer tests usually involve human operations and become somewhat impractical when the damping of the system is huge. For harmonic excitations, the excitation frequency is commonly fixed. Papers [11,28,32] reported that different excitation frequencies have different diagnostic performances for big and small cracks. This means that fixed excitation frequency may not be enough for all situations. There is an alternative but forsaken way, namely sweep excitation, that can be used to discover the non-linear dynamic properties of a beam. Giannini et al. [17,34] found that more solid crack detection results can be obtained by using a slow-varying sweep excitation. However, their sweep ranged only a few Hz around the resonance frequency. Referring to the start-up operations that are usually implemented to diagnose faults in rotating machines [35], a wider sweep excitation range for beams may capture richer non-linearity information relevant to crack. In this paper, we will explore the benefits of using a wider sweep range to detect breathing cracks.

Apart from non-linearities, sweep excitations induce non-stationarities in vibration responses. This makes it hard to retrieve frequency harmonics with normal Fourier Transforms (FT). Order Tracking (OT) is an effective solution to non-stationary signals and has been successfully used for diagnosing rotating machines [36,37]. Typical OT techniques include Computed OT (COT) [38], Vold-Kalman Filtering OT [39] and etc. Among them, COT gives us order domain spectrum that are similar to frequency spectrum. It resamples the signals by a constant rotational angle increment and uses the main shaft rotating frequency as the reference to track the signal contents. The ratio of a frequency to the main shaft rotating frequency is called order. In order spectrum, order harmonics can be graphed and are potential non-linear features for crack detection. In our previous work [40], we adopted the angular resampling in COT for processing beam vibration signals. Based on this, we can track the order harmonics of beam vibrations under sweep excitations and utilize them as features for beam crack evaluation.

To summarize, extracting non-linear features from vibrational signals are important in beam crack status evaluation. Sweep excitation and harmonics are effective ways to respectively energize and capture the non-linearities introduced by crack. Using the resampling idea in COT, non-linear order harmonics can be retrieved from the beam's vibrations under sweep excitations. In this paper, we aim to investigate the effectiveness of order harmonics in beam crack evaluation, and we also study the details of extracting harmonics from spectrum. The contributions of this paper can be highlighted as follows:

1. Sweep excitation across many Hz is implemented to capitalize on the non-linearity introduced by breathing cracks;
2. Order spectrum for beam vibrations are constructed and window based harmonics extracting techniques are studied for crack evaluations;
3. Experimental data together with Support Vector Machines (SVMs) are used to assess the ability of extracted harmonics in evaluating cracks.

Remaining parts are organized as follows: Section 2 introduces related theories, Section 3 proposes the diagnostic method. Section 4 gives experimental demonstration and discussions of the proposed method. Finally, Section 5 concludes this study.

2. Related theory

2.1. Crack breathing non-linearity

The deflection of a simply supported beam, as shown in Fig. 1, under harmonic excitation can be written as:

$$x(t) = A(\omega) \sin \omega t \quad (2.1)$$

$$A(\omega) = \frac{2f_0}{\rho d \Pi} \sum_{n=1}^{\infty} \frac{1}{\omega_n^2 - \omega^2} \sin \frac{n\pi l}{L} \sin \frac{n\pi d}{L} \quad (2.2)$$

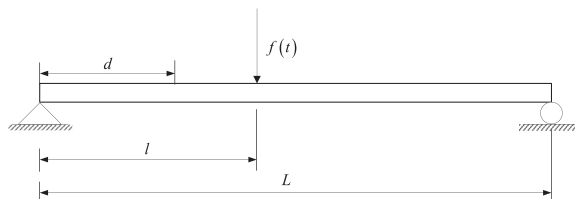


Fig. 1. Simply supported beam under excitation.

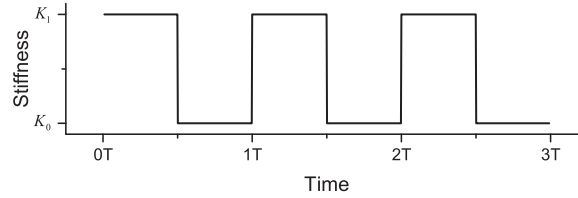


Fig. 2. Stiffness curve of the beam with a breathing crack.

where ω is the angular excitation frequency, f_0 is the excitation amplitude, d is the coordinate of the observation point, l is the coordinate of the excitation point, L is the length of the beam (Fig. 1), t stands for time, ρ is mass density, Π is area of cross-section and ω_n is the n th angular natural frequency.

Consider a simply supported beam with a crack as a simple Single Degree-of-Freedom (SDoF) system with time-variant stiffness as treated by Saavedra and Cuitio [15]. The equation of motion and its solution under a periodic driving force can be written as:

$$m\ddot{x} + c\dot{x} + k(t)x = f(t) \tag{2.3}$$

where m is mass, c is damping, $k(t)$ is the time-variant stiffness, and $f(t)$ is the external excitation force.

The curve of $k(t)$ versus t is shown in Fig. 2, where K_0 is the stiffness when the crack is open, K_1 is the stiffness when the crack is closed, and T is the period of the periodic excitation force. Note $k(t)$ can be expanded with Fourier Series as:

$$k(t) = \frac{K_1 + K_0}{2} + \frac{2\Delta K}{\pi} \sum_{i=1}^{\infty} \frac{1}{2i-1} \sin \frac{2\pi(2i-1)t}{T} \tag{2.4}$$

where $\Delta K = K_1 - K_0$.

With $k(t)$ of Equation (2.4), (2.3) can be transformed into:

$$m\ddot{x} + c\dot{x} + \frac{K_1 + K_0}{2}x = f(t) - \frac{2\Delta K}{\pi} \sum_{i=1}^{\infty} \frac{x}{2i-1} \sin \frac{2\pi(2i-1)t}{T} \tag{2.5}$$

which can be solved by using an iterative method [41]. Without loss of generality, let the external excitation force $f(t) = \sin \omega t$, where $\omega = \frac{2\pi}{T}$. Using a superscript with parentheses to denote the number of iteration, the first approximate solution of x is expressed as [41]:

$$x^{(1)} = A^{(1)} \sin \omega t \tag{2.6}$$

and the first approximate total excitation, that is, the right hand side of Equation (2.5), is:

$$f^{(1)}(t) = f(t) - \frac{2\Delta K}{\pi} \sum_{i=1}^{\infty} \frac{x^{(1)} \sin(2i-1)\omega t}{2i-1} \tag{2.7}$$

$$= f(t) + \frac{A^{(1)}\Delta K}{\pi} \sum_{i=1}^{\infty} \frac{\cos 2i\omega t - \cos 2(i-1)\omega t}{2i-1} \tag{2.8}$$

From Equation (2.8), it can be seen that even harmonics are present in the total excitation. Hence, the second approximation of x can be expressed as [41]:

$$x^{(2)} = x^{(1)} + \sum_{j=1}^{\infty} A_j^{(2)} \cos 2j\omega t \tag{2.9}$$

Iteratively, the second approximate total excitation is:

$$\begin{aligned} f^{(2)}(t) &= f(t) - \frac{2\Delta K}{\pi} \sum_{i=1}^{\infty} \frac{x^{(2)} \sin(2i-1)\omega t}{2i-1} \\ &= f(t) - \frac{2\Delta K}{\pi} \sum_{i=1}^{\infty} \left(x^{(1)} + \sum_{j=1}^{\infty} A_j^{(2)} \cos 2j\omega t \right) \frac{\sin(2i-1)\omega t}{2i-1} \\ &= f^{(1)}(t) - \frac{2\Delta K}{\pi} \sum_{i=1}^{\infty} \frac{\sin(2i-1)\omega t}{2i-1} \sum_{j=1}^{\infty} A_j^{(2)} \cos 2j\omega t \end{aligned}$$

$$\begin{aligned}
 &= f^{(1)}(t) - \frac{2\Delta K}{\pi} \sum_{i=1}^{\infty} \sum_{j=1}^{\infty} \frac{A_j^{(2)}}{2i-1} \sin(2i-1)\omega t \cos 2j\omega t \\
 &= f^{(1)}(t) - \frac{\Delta K}{\pi} \sum_{i=1}^{\infty} \sum_{j=1}^{\infty} \frac{A_j^{(2)}}{2i-1} [\sin(2i+2j-1)\omega t + \sin(2i-2j-1)\omega t]
 \end{aligned}$$

Form this equation, it can be seen that the right hand side of the equation of motion contains both even and odd harmonics. This means that the solution of this equation will also have both even and odd harmonics and this solution could be written as:

$$x = \sum_{k=1}^{\infty} A_k \sin k\omega t \tag{2.10}$$

where A_k is the amplitude of the k th harmonic (A_1 is the amplitude of the base frequency).

For frequency sweep excitations, the angular excitation frequency ω is a function of time. A_k s are combinations of $A(\omega)$ s in Equation (2.2), and should also be functions of time. This means that A_k s have these three properties as $A(\omega)$ s do:

- 1) A_k s are related to the crack breathing non-linearity owing to their dependence on the time-variant stiffness values;
- 2) The values of A_k s are a summation of many components in the solution and are non-linear for crack status;
- 3) A_k s are functions of the excitation frequency and should be time-variant if the excitation frequency is so.

For the response under frequency sweep excitation, according to Equation (2.2), the vibration amplitude should be high when the frequency is close to the natural frequencies and low when it is not.

2.2. Computed order tracking

Computed order tracking is commonly used order tracking technique which utilizes the order spectrum to represent the non-stationary vibration signals [42]. Essentially, it first uses angular resampling and interpolation to reconstruct the vibration signal using constant angular increments. Then, the order spectrum, the angular counterpart of the common frequency spectrum, can be obtained by applying Fourier Transform to the reconstructed signal. The computation of this process can be written as [43]:

$$X[m] = \frac{1}{N} \sum_{n=0}^{N-1} x[n\Delta\theta] e^{-jo[m]n\Delta\theta} \tag{2.11}$$

where $X[m]$ is the order amplitude at the m th point in the order spectrum, N is the number of data points of the signal x , $\Delta\theta$ is the constant angular increment and $o[m]$ is the order value at the m th point in the order spectrum. Specifically, $x[n\Delta\theta]$ is reconstructed by resampling and interpolating the raw time series x . The detailed process will be explained in section 3.

A crucial step for reconstructing the angular signal is to determine the swept angle of the external excitation. Commonly, for rotating machinery, it is determined with reference of rotating speed of the main shaft. Here, in the case of beam vibration, the excitation frequency can be utilized as the reference and be regard as the first order in the order spectrum. The oscillation of the

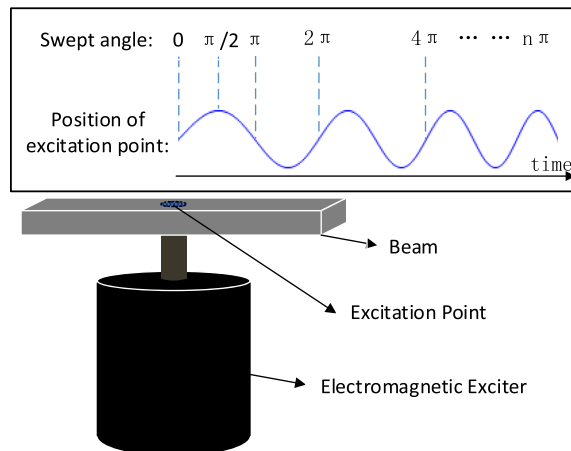


Fig. 3. Vibration of the excitation point and the swept angle versus time.

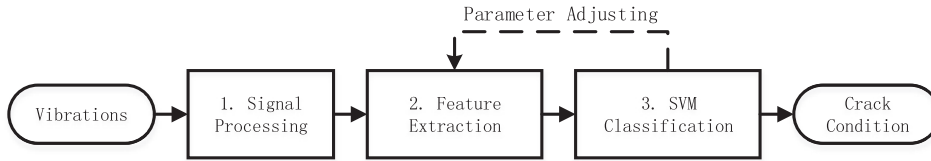


Fig. 4. Schematic of the proposed beam crack status classification method.

excitation point and illustration of the swept angle are shown in Fig. 3. For the sweep excitation case that the angular excitation frequency $\omega(t) = 2\pi at$, the swept angle can be calculated as:

$$\theta(t) = \int \omega(t) dt = \pi at^2 \quad (2.12)$$

In other words, the swept angle is a quadratic function of time.

3. Proposed method

Based on COT and SVMs, we propose a novel method to detect crack and evaluate its depth using the collected vibration response under sweep excitations. Firstly, the order tracking technique is applied to get the order spectrum of the collected signals. Secondly, multiple features are extracted and selected from the obtained order spectrum to represent the respective vibration pattern. Lastly, multi-class SVMs are trained to map the selected features to the labelled crack status and are tested to adjust the parameters of feature extraction process. The schematic of the proposed method is shown in Fig. 4.

3.1. Signal reconstruction

To begin with, as a data-driven approach, this method involves processing a large amount of vibration signals that are collected during multiple runs of the excitations. In practice, there are usually many factors, such as mounting errors, that usually cause measurement errors. In this study, a normalization of the data across all time points are performed to mitigate such possible effects. All signals are shifted to zero means and scaled to unit variance using Equation (3.1).

$$s = \frac{s_{original} - \mu_s}{\sqrt{\sigma_s}} \quad (3.1)$$

where s is the normalized signal, $s_{original}$ is the original signal, μ_s is the mean value of $s_{original}$ across all time points and σ_s is the variance of $s_{original}$.

In sweep excitation, the excitation force has a constant amplitude while its frequency linearly grows within a certain time length. At a certain point on the beam, the vibration response is collected by a single accelerometer for further analysis. It should be noted that both the excitation frequency and the amplitude of the response are time-variant. Under such circumstances, the beam experiences a range of vibration states instead of fixed ones, which can be beneficial for identifying crack status. However, difficulties are introduced in processing vibration signals and appropriate faulty feature extraction techniques are required.

Considering that analogy between the external excitation to the beams and the drive shaft of a rotating machinery, the authors borrow some insights from COT for diagnosis in gears and bearings. For gears and bearings, computed order tracking utilizes the measured rotating speed information to resample and interpolate the vibration data at constant angular intervals before applying Fourier Transform. For beams, the excitation frequency can be regarded as the “rotating speed” and the relative displacement as the “rotation angle”. Fig. 5 gives an illustration of the quadratic relationship between the swept angles with time, and a demonstration to determine the resampling and interpolating time points. The angular reconstruction process is described as follows:

- i. Locate the angular points which are the points when the swept angle increases by 2π rads comparing to the previous angular points or the starting point;
- ii. Mark the resample points by using the indices of angular points and I interpolation points between neighbor angular points ($I + 1$ resample points for every 2π rads);
- iii. Reconstruct the vibration signal by splining the resampled points of raw signal.

In the end, the order spectrum of raw vibration signals can be obtained by applying FT to the reconstructed signals. The maximum order o_{max} in order spectrum is $\frac{I+1}{2}$.

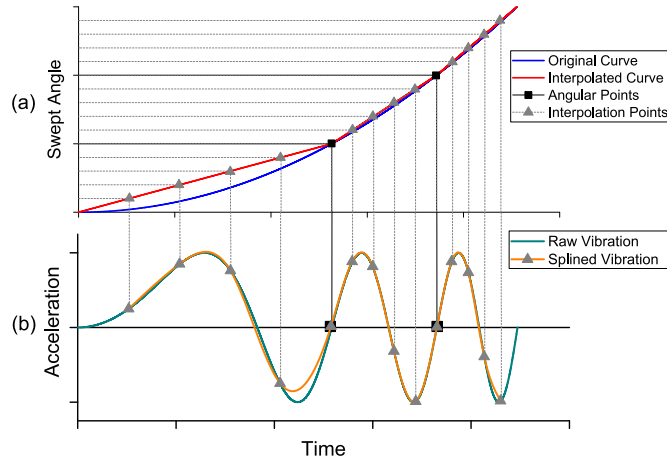


Fig. 5. Illustration of the signal reconstruction process.

3.2. Feature extraction

Similar to the frequency spectrum, the order spectrum is organized as the amplitudes of different orders of the signal. For vibration signals of beams, the amplitudes should be prominent at integer orders according to Equation (2.10). The amplitudes at integer orders are appropriate and accessible features to indicate crack status. However, these amplitudes cannot be directly read due to the limited resolution of the order spectrum. Amplitude distortion and smearing effect often exist in the spectrum due to a series of numerical operation, e.g. numerical integration and interpolation. Consequently, the amplitude at a single order point is not ideal to reflect the true value of an order content. Alternatively, the approximate values can be extracted as faulty features range by considering all local spectrum amplitudes within an appropriate range.

In this paper, firstly, rectangle windows are applied to mask the order spectrum. Then the p -norm is utilized to convert the masked one dimensional order vectors into scalars as features. To be specific, let Λ denotes an order vector that contains all the amplitudes in an order spectrum with M order points and the maximum order o_{max} . The order resolution, similar to frequency resolution in frequency spectrum, is then $\Delta o = \frac{o_{max}}{M}$. The i th element in the vector of the rectangle window centered at order n is set as:

$$W_{\psi}^n [i] = \begin{cases} 1, & \frac{n - 0.5\psi}{\Delta o} \leq i < \frac{n + 0.5\psi}{\Delta o} \\ 0, & \text{other } i \end{cases} \tag{3.2}$$

where ψ is the width of the window. Finally, the n^{th} feature can be calculated as:

$$f_p^n = \left\| W_{\psi}^n \Lambda \right\|_p \tag{3.3}$$

where the operation $\| \cdot \|_p$ is to calculate the p -norm of a vector. In this paper, p is chosen from 1, 2 and ∞ . Note that 1-norm, or L_1 -norm, is the sum of the absolute values of the vector. The 2-norm, or L_2 -norm, returns the Euclidean length of the vector. The ∞ -norm, or max-norm, gives the maximum absolute value of all elements in the vector.

3.3. SVM classification

SVMs have been proved to be effective both for regression problems [44] and classification problems [45] in different areas. In this study, the diagnosis of beam crack is treated as a pattern recognition task by discretizing the crack status into different levels. One-Against-One SVMs [46], or OAO SVMs, with linear kernel are applied to map the features to labels of crack status. The input feature matrix is constructed as $X_p^N = (\overline{f}_p^1 \ \overline{f}_p^2 \ \dots \ \overline{f}_p^N)$, where \overline{f}_p^n contains the n^{th} feature of all data samples and all feature vectors are normalization via Equation (3.4).

$$f_p^n = \frac{f_p^n - \text{mean}(\overline{f}_p^n)}{\sqrt{\text{var}(\overline{f}_p^n)}} \tag{3.4}$$

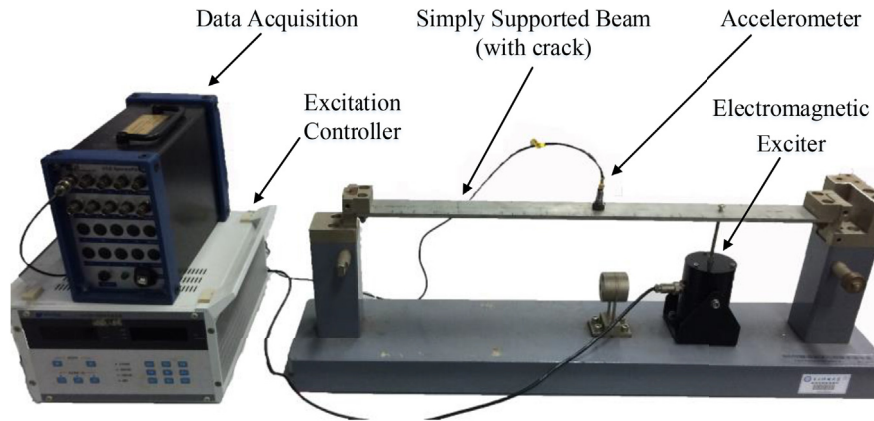


Fig. 6. Experimental test rig.

Table 1
Geometric parameters and material properties of the simply supported beam.

Beam Structural Parameter	Value
Length	587.5 mm
Width	50.0 mm
Thickness	5.5 mm
Crack location	128 mm
Material	Aluminum

The quality of the diagnosis is evaluated by the Cross Validation (CV) [47] accuracy and the optimal parameters (p and N) can be determined by looking for the highest k -fold CV accuracy with a grid search. At the same time, the best SVM model yielding the highest diagnosis accuracy can be obtained.

4. Experimental study

To show the effectiveness and demonstrate the procedures of the proposed method, experiments are carried out on simply supported beams with different crack levels.

4.1. Experimental settings

The experimental test rig in Fig. 6 includes a simply supported beam setup, a data acquisition system, an accelerometer, an electromagnetic exciter, and an excitation controller. Table 1 gives a specific description to the simply supported beam. Fig. 7 gives the different crack levels of the beam. The seeded cracks are artificially made by electric discharge machining and are spanned across the transverse direction of the beam. The location of the crack is the same. Only the crack depth are different. The accelerometer is mounted at the center of the beams surface as it is shown in Fig. 6.

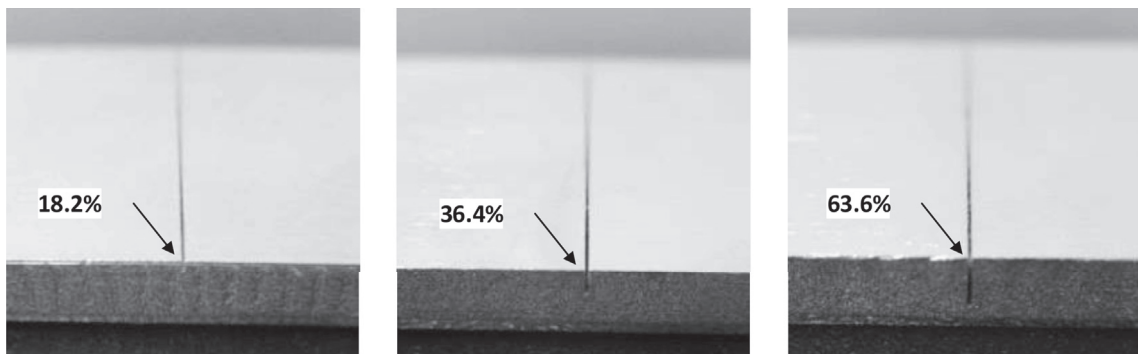


Fig. 7. Three different relative depths of beam cracks.

Table 2

Description to all excitation settings.

Exciter input voltage	2v		0.1v	
Excitation frequency	$2\pi \times 5$ tHz	$2\pi \times 20$ Hz	$2\pi \times 20$ tHz	$2\pi \times 20$ Hz
Notation	SWET-2v	COET-2v	SWET-01v	COET-01v

Sweep excitation (SWET) and proposed method are implemented to detect crack and its depth. At the same time, constant frequency excitation (COET) and similar feature extraction methods are also performed for comparisons. Besides, two exciter input voltage are tested to investigate the performance of the proposed method under different amplitude levels of excitation forces. All tested excitation settings and their notation are listed in Table 2. For SWET signals, the interpolation point number I (see in Section 3.1) is set to be 19, which means that σ_{\max} is 10. Thus the number of input features N is varying from 1 to 9 (the 10th feature is not available for that it involves orders greater than 10). The window size ψ is set to be 0.1. For COET signals, similar to SWET, amplitudes of harmonics in the frequency spectrum are extracted as features. Different from the order spectrum, in the frequency spectrum, the windows are centered at multiples of the excitation frequency and sized as 0.1 times the excitation frequency. Alternatively, one can rescale the frequency axis before applying the identical feature extraction method as in SWET scenarios instead of re-sizing the window. In total, 108 different feature matrices (4 excitation scenarios, 3 norm operations, 9 feature numbers) will be fed into SVMs and different CV accuracies can be obtained.

All signal samples are collected with a sampling frequency of 2560Hz and 24 s in length. For each excitation scenario, 240 signal samples (60 for each crack level) are collected. To get unbiased validation accuracies, 20 rounds of 10-fold CV are run and the validation accuracies are averaged over the rounds.

4.2. Results and discussions

Firstly, 4 signal examples (from perfect beams without crack) and their order spectrum or frequency spectrum in 4 different excitation scenarios are shown in Fig. 8. Fig. 8(a), (c), (e) and (g) are, respectively, the time domain signals of COET-01v, COET-2v, SWET-01v, and SWET-2v. Fig. 8(b) and (d) are the frequency spectrums of (a) and (c), respectively. Fig. 8(f) and (h) are the order spectrums of (e) and (g), respectively. All the y axes of the frequency spectra and the order spectra are logarithmic. It should be noted that all signals will be normalized across time as in Equation (3.1).

From Fig. 8, it can be seen that:

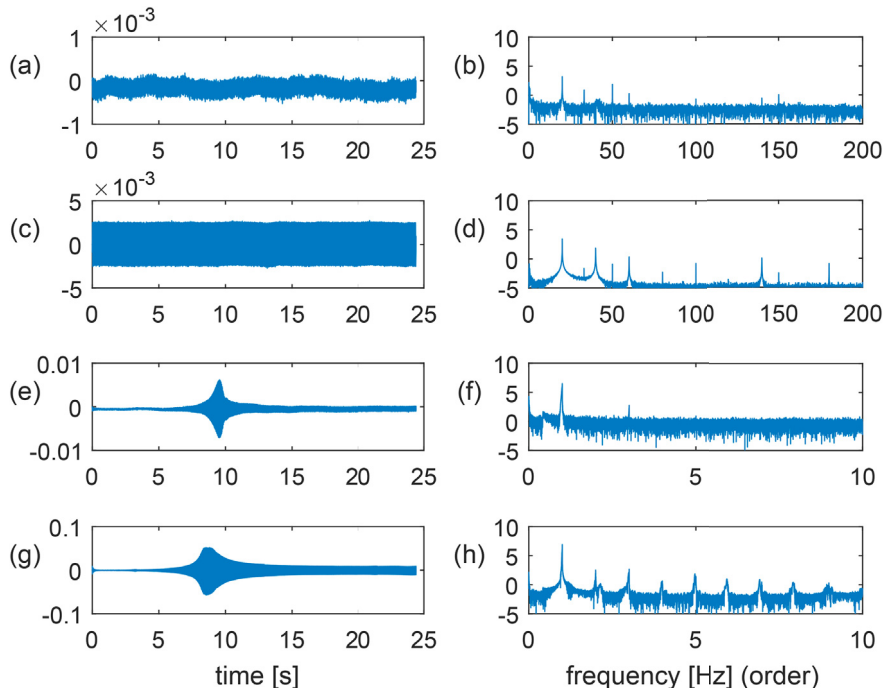


Fig. 8. Signal examples of 4 excitation scenarios.

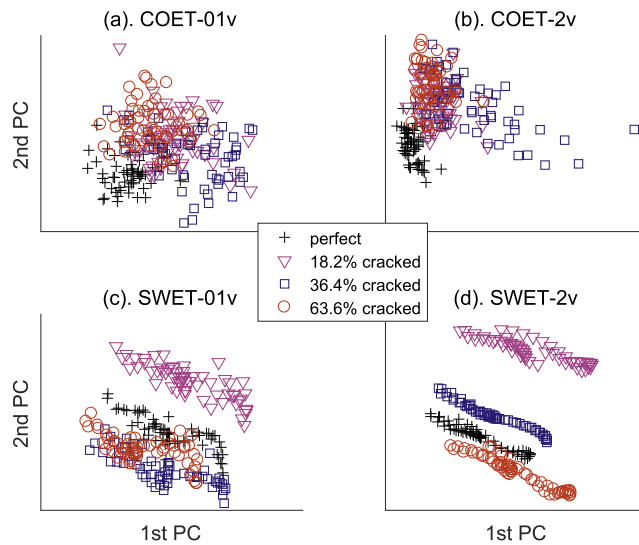


Fig. 9. First 2 PCs of max-norm features.

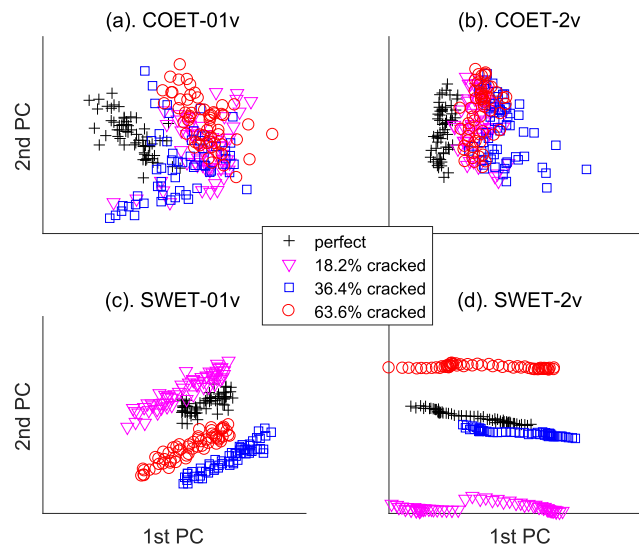


Fig. 10. First 2 PCs of L_1 -norm features.

- 1). The vibration amplitude is stable under COETs while bell-shape envelopes are obtained under SWETs;
- 2). Harmonics are present in both frequency spectra and order spectra and more harmonics are present at higher excitation input as in (d) and (h);
- 3). Spectral leakage to neighbouring frequencies or orders can be observed, especially in (h), and the noise floor is higher when using small excitations ((b) and (f)).

Based on the above observations, it is promising to extract features from harmonics or integer orders. Besides, considering the spectral smearing effect, the windowing scheme in Section 3.2 that takes multiple spectral points into consideration is also reasonable.

To visualize the capabilities of the extracted features to represent different crack levels, principal component analysis (PCA) is applied to transform high dimensional feature matrices to principal components (PCs). In total, 12 groups of first 2 PCs of different X_p^0 s are plotted in Fig. 9 (max-norm), Fig. 10 (L_1 -norm) and Fig. 11 (L_2 -norm). In each Figure, (a), (b), (c) and (d) stands for 4 different excitation scenarios.

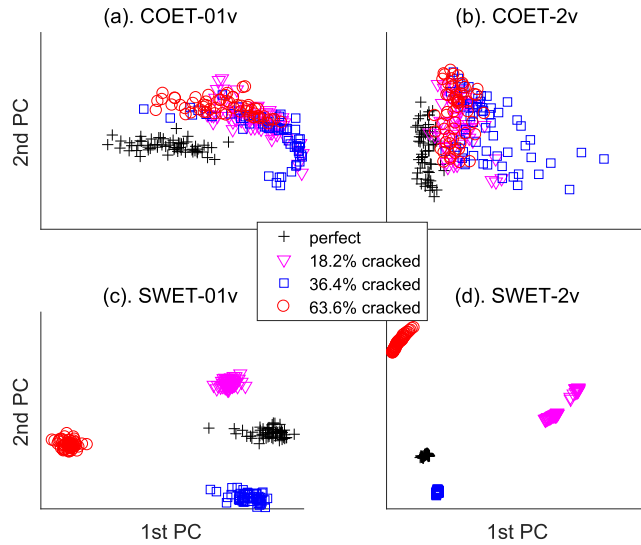


Fig. 11. First 2 PCs of L_2 -norm features.

From Figs. 9–11, it can be seen that crack levels are clearly separable in Fig. 11(c) and (d). PCs of samples with different labels in Figs. 9(d), 10(c) and (d) are also separated. However, in other scatter plots, the label overlapping are evident. In general, features from order spectra are more indicative to crack level than ones from frequency spectra. In those good PC planes, samples with the same label are more shattered when the excitation input is low. Specifically, by regarding to the PC planes, SWET-2 with L_2 -norm operation (Fig. 11(d)) is the best choice to evaluate beam crack levels.

Lastly, an assessment to all the aforementioned settings, including the number of features to be extracted, is given. For that, all CV accuracies resulting from 108 feature matrices are shown in Fig. 12 (2v input voltage) and Fig. 13 (0.1v input voltage).

In both Figs. 12 and 13, SWETs are much better than COETs and the L_2 -norm results the highest accuracy with other settings at the same levels. Under COETs, the best SVM model is attained when $N = 6$, $p = L_1$ and input voltage is 2v. However, the accuracy bars are still very low comparing SVM to most CV accuracies from SWET. In the cases that the excitation input is high

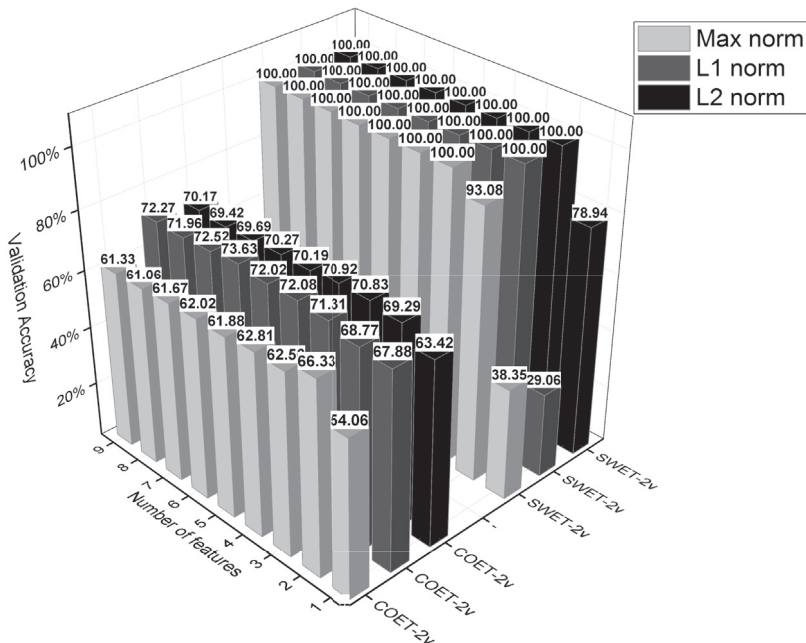


Fig. 12. Classification accuracies with 2v excitation input.

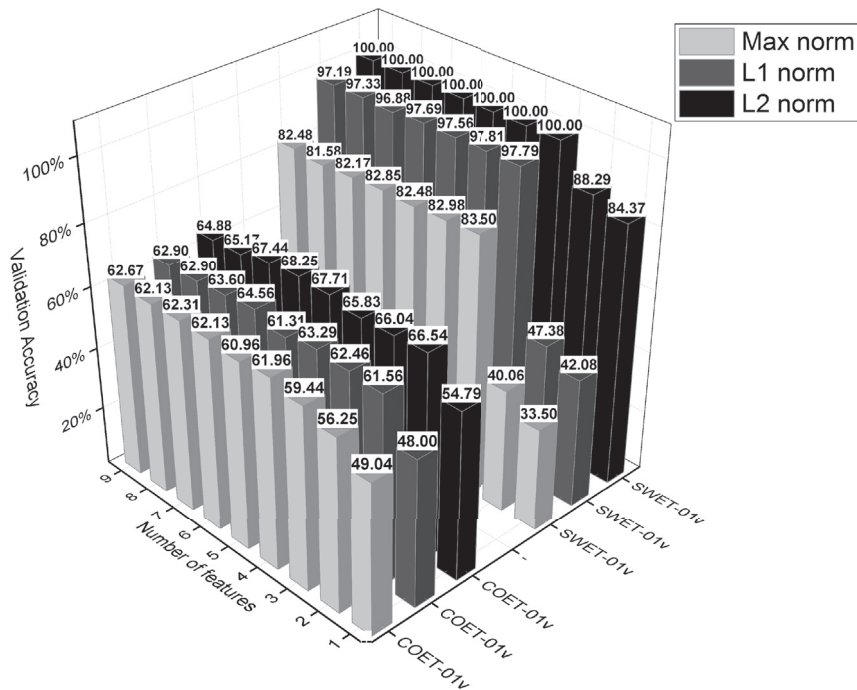


Fig. 13. Classification accuracies with 0.1v excitation input.

enough and more than two features are considered, the difference of using different norm operations becomes negligible. The overall validation accuracy drops with the excitation input voltage. SWET-2v plus L_2 -norm operation can still give us solid predictions if only the first 3 features are available. Recalling that in Fig. 8(f), only the amplitudes at the first and the third orders are prominent, it can be said that these two order contents are vital for evaluating crack level of simply supported beam.

5. Conclusion

The proposed method is effective for crack depth evaluation as the classification accuracies of all SVM models achieves 100%. The results show that vibration response from sweep excitation is more effective than that from constant frequency excitation. Apart from this, the excitation input voltage and the feature extraction scheme are also crucial for diagnosis accuracy. Generally, larger excitations to beams are preferred for evaluating the depth of the crack and L_2 -norm $>$ L_1 -norm $>$ max-norm for windowing feature extraction. We can also know that the first three order contents are very important for beam crack evaluation.

While clear classification is obtained in this case study, the non-linear progression of sample clusters corresponding to crack depths (Figs. 9–11) is an issue. Additional data are needed covering a wider range of crack levels. That is, more damage scenarios must be studied. Data driven methods can be used for more effective classification. In addition, COT based features proposed in this paper and features based on other domain knowledge, for instance, fracture mechanic knowledge, are beneficial for improving the capability of such data drive approaches.

Apart from above, many further investigations can be conducted including but not limited to 1) focus on other diagnostic tasks like evaluating smaller cracks and their locations; 2) develop the proposed method by adjusting the speed-up rate of sweep excitations and window size of feature extraction.

Acknowledgement

This research is supported by the National Key Research and Development Program of China (Project No. 2017YFC0108401), Fundamental Research Funds for the Centred University (ZYGX2016J111), and National Science Foundation of China (51305067).

References

- [1] Y. Yao, S.T.E. Tung, B. Glisic, Crack detection and characterization techniques—An overview, Struct. Contr. Health Monit. 21 (12)(2014) 1387–1413, <https://doi.org/10.1002/stc.1655>.
- [2] R.B. Randall, Introduction and Background. in: Vibration-based Condition Monitoring, John Wiley & Sons, Ltd., 2011, ISBN: 978-0-470-97766-8, pp. 1–23.
- [3] Y.J. Yan, L. Cheng, Z.Y. Wu, L.H. Yam, Development in vibration-based structural damage detection technique, Mech. Syst. Signal Process. 21 (5) (2007) 2198–2211, <https://doi.org/10.1016/j.ymssp.2006.10.002>.

- [4] E.P. Carden, P. Fanning, Vibration based condition monitoring: a review, *Struct. Health Monit.* 3 (4) (2004) 355–377, <https://doi.org/10.1177/1475921704047500>.
- [5] K. Zhang, X. Yan, Multi-cracks identification method for cantilever beam structure with variable cross-sections based on measured natural frequency changes, *J. Sound Vib.* 387 (2017) 53–65, <https://doi.org/10.1016/j.jsv.2016.09.028>.
- [6] N.T. Khiem, L.K. Toan, A novel method for crack detection in beam-like structures by measurements of natural frequencies, *J. Sound Vib.* 333 (18) (2014) 4084–4103, <https://doi.org/10.1016/j.jsv.2014.04.031>.
- [7] M.K. Sutar, S. Pattanaik, J. Rana, Neural based controller for smart detection of crack in cracked cantilever beam, *Mater. Today: SAVE Proc.* 2 (4) (2015) 2648–2653, <https://doi.org/10.1016/j.matpr.2015.07.225>.
- [8] H.Y. Guo, Structural damage detection using information fusion technique, *Mech. Syst. Signal Process.* 20 (5) (2006) 1173–1188, <https://doi.org/10.1016/j.ymssp.2005.02.006>.
- [9] R.A. Saeed, A.N. Galybin, V. Popov, Crack identification in curvilinear beams by using ANN and ANFIS based on natural frequencies and frequency response functions, *Neural Comput. Appl.* 21 (7) (2012) 1629–1645, <https://doi.org/10.1007/s00521-011-0716-1>.
- [10] A.D. Dimarogonas, Vibration of cracked structures: a state of the art review, *Eng. Fract. Mech.* 55 (5) (1996) 831–857, [https://doi.org/10.1016/0013-7944\(94\)00175-8](https://doi.org/10.1016/0013-7944(94)00175-8).
- [11] A. Bovsunovsky, C. Surace, Non-linearities in the vibrations of elastic structures with a closing crack: a state of the art review, *Mech. Syst. Signal Process.* 6263 (2015) 129–148, <https://doi.org/10.1016/j.ymssp.2015.01.021>.
- [12] J.K. Sinha, M.I. Friswell, S. Edwards, Simplified models for the location of cracks in beam structures using measured vibration data, *J. Sound Vib.* 251 (1) (2002) 13–38, <https://doi.org/10.1006/jjsvi.2001.3978>.
- [13] N. Dharmaraju, R. Tiwari, S. Talukdar, Identification of an open crack model in a beam based on force-response measurements, *Comput. Struct.* 82 (2) (2004) 167–179, <https://doi.org/10.1016/j.compstruc.2003.10.006>.
- [14] X. Zhang, R.X. Gao, R. Yan, X. Chen, C. Sun, Z. Yang, Multivariable wavelet finite element-based vibration model for quantitative crack identification by using particle swarm optimization, *J. Sound Vib.* 375 (2016) 200–216, <https://doi.org/10.1016/j.jsv.2016.04.018>.
- [15] P.N. Saavedra, L.A. Cuitiño, Crack detection and vibration behavior of cracked beams, *Comput. Struct.* 79 (16) (2001) 1451–1459, [https://doi.org/10.1016/S0045-7949\(01\)00049-9](https://doi.org/10.1016/S0045-7949(01)00049-9).
- [16] J.K. Sinha, M.I. Friswell, Simulation of the dynamic response of a cracked beam, *Comput. Struct.* 80 (18) (2002) 1473–1476, [https://doi.org/10.1016/S0045-7949\(02\)00098-6](https://doi.org/10.1016/S0045-7949(02)00098-6).
- [17] O. Giannini, P. Casini, F. Vestroni, Nonlinear harmonic identification of breathing cracks in beams, *Comput. Struct.* 129 (2013) 166–177, <https://doi.org/10.1016/j.compstruc.2013.05.002>.
- [18] A.C. Neves, F.M.F. Simões, A.P.d. Costa, Vibrations of cracked beams: discrete mass and stiffness models, *Comput. Struct.* 168 (2016) 68–77, <https://doi.org/10.1016/j.compstruc.2016.02.007>.
- [19] T.G. Chondros, A.D. Dimarogonas, J. Yao, Vibration of a beam with a breathing crack, *J. Sound Vib.* 239 (1) (2001) 57–67, <https://doi.org/10.1006/jjsvi.2000.3156>.
- [20] S.D. Nguyen, K.N. Ngo, Q.T. Tran, S.B. Choi, A new method for beam-damage-diagnosis using adaptive fuzzy neural structure and wavelet analysis, *Mech. Syst. Signal Process.* 39 (12) (2013) 181–194, <https://doi.org/10.1016/j.ymssp.2013.03.023>.
- [21] K.V. Nguyen, Mode shapes analysis of a cracked beam and its application for crack detection, *J. Sound Vib.* 333 (3) (2014) 848–872, <https://doi.org/10.1016/j.jsv.2013.10.006>.
- [22] M.T. Vakil-Baghmisheh, M. Peimani, M.H. Sadeghi, M.M. Etefagh, Crack detection in beam-like structures using genetic algorithms, *Appl. Soft Comput.* 8 (2) (2008) 1150–1160, <https://doi.org/10.1016/j.asoc.2007.10.003>.
- [23] G.M. Owolabi, A.S.J. Swamidias, R. Seshadri, Crack detection in beams using changes in frequencies and amplitudes of frequency response functions, *J. Sound Vib.* 265 (1) (2003) 1–22, [https://doi.org/10.1016/S0022-460X\(02\)01264-6](https://doi.org/10.1016/S0022-460X(02)01264-6).
- [24] S. Loutridis, E. Douka, A. Trochidis, Crack identification in double-cracked beams using wavelet analysis, *J. Sound Vib.* 277 (45) (2004) 1025–1039, <https://doi.org/10.1016/j.jsv.2003.09.035>.
- [25] J.T. Kim, N. Stubbs, Crack detection in beam-type structures using frequency data, *J. Sound Vib.* 259 (1) (2003) 145–160, <https://doi.org/10.1006/jjsvi.2002.5132>.
- [26] L. Gelman, S. Gorpnich, C. Thompson, Adaptive diagnosis of the bilinear mechanical systems, *Mech. Syst. Signal Process.* 23 (5) (2009) 1548–1553, <https://doi.org/10.1016/j.ymssp.2009.01.007>.
- [27] Z.K. Peng, Z.Q. Lang, S.A. Billings, Crack detection using nonlinear output frequency response functions, *J. Sound Vib.* 301 (35) (2007) 777–788, <https://doi.org/10.1016/j.jsv.2006.10.039>.
- [28] A.P. Bovsunovsky, C. Surace, Considerations regarding superharmonic vibrations of a cracked beam and the variation in damping caused by the presence of the crack, *J. Sound Vib.* 288 (45) (2005) 865–886, <https://doi.org/10.1016/j.jsv.2005.01.038>.
- [29] F. Lonard, J. Lanteigne, S. Lalonde, Y. Turcotte, Free-vibration behaviour of a cracked cantilever beam and crack detection, *Mech. Syst. Signal Process.* 15 (3) (2001) 529–548, <https://doi.org/10.1006/mssp.2000.1337>.
- [30] L. Gelman, S. Gorpnich, Non-linear vibroacoustical free oscillation method for crack detection and evaluation, *Mech. Syst. Signal Process.* 14 (3) (2000) 343–351, <https://doi.org/10.1006/mssp.1999.1236>.
- [31] U. Andreaus, P. Casini, F. Vestroni, Non-linear dynamics of a cracked cantilever beam under harmonic excitation, *Int. J. Non Lin. Mech.* 42 (3) (2007) 566–575, <https://doi.org/10.1016/j.ijnonlinmec.2006.08.007>.
- [32] U. Andreaus, P. Baragatti, Experimental damage detection of cracked beams by using nonlinear characteristics of forced response, *Mech. Syst. Signal Process.* 31 (2012) 382–404, <https://doi.org/10.1016/j.ymssp.2012.04.007>.
- [33] N. Wu, Study of forced vibration response of a beam with a breathing crack using iteration method, *J. Mech. Sci. Technol.* 29 (7) (2015) 2827–2835, <https://doi.org/10.1007/s12206-015-0611-2>.
- [34] O. Giannini, P. Casini, F. Vestroni, Nonlinear harmonic identification of cracks in structures, in: *Dynamics of Civil Structures, Volume 4. Conference Proceedings of the Society for Experimental Mechanics Series*, Springer, Cham, 2014, pp. 207–217, https://doi.org/10.1007/978-3-319-04546-7_24.
- [35] M. Silani, S. Ziaei-Rad, H. Talebi, Vibration analysis of rotating systems with open and breathing cracks, *Appl. Math. Model.* 37 (24) (2013) 9907–9921, <https://doi.org/10.1016/j.apm.2013.05.040>.
- [36] K.S. Wang, P.S. Heyns, The combined use of order tracking techniques for enhanced Fourier analysis of order components, *Mech. Syst. Signal Process.* 25 (3) (2011) 803–811, <https://doi.org/10.1016/j.ymssp.2010.10.005>.
- [37] P. Borghesani, P. Pennacchi, R.B. Randall, R. Ricci, Order tracking for discrete-random separation in variable speed conditions, *Mech. Syst. Signal Process.* 30 (2012) 1–22, <https://doi.org/10.1016/j.ymssp.2012.01.015>.
- [38] K.R. Fyfe, E.D.S. Munck, Analysis of computed order tracking, *Mech. Syst. Signal Process.* 11 (2) (1997) 187–205, <https://doi.org/10.1006/mssp.1996.0056>.
- [39] K.S. Wang, D. Guo, P.S. Heyns, The application of order tracking for vibration analysis of a varying speed rotor with a propagating transverse crack, *Eng. Fail. Anal.* 21 (2012) 91–101, <https://doi.org/10.1016/j.engfailanal.2011.11.020>.
- [40] K. Wang, Y. Wang, D. Luo, Q. He, Application of order tracking rationale to non-rotating cantilever beam analysis, in: *2014 International Conference on Prognostics and Health Management*, 2014, pp. 1–6, <https://doi.org/10.1109/ICPHM.2014.7036365>.
- [41] S. Rao, *Mechanical Vibrations*, Prentice Hall, 2004, ISBN: 0130489875.
- [42] K. Feng, K. Wang, P. Chen, A signal selection scheme through order tracking techniques for planetary gearbox condition monitoring, in: *Prognostics and System Health Management Conference (PHM-Chengdu)*, 2016, IEEE, 2016, pp. 1–5, <https://doi.org/10.1109/PHM.2016.7819880>.
- [43] P. Borghesani, P. Pennacchi, S. Chatterton, R. Ricci, The velocity synchronous discrete Fourier transform for order tracking in the field of rotating machinery, *Mech. Syst. Signal Process.* 44 (12) (2014) 118–133, <https://doi.org/10.1016/j.ymssp.2013.03.026> Special Issue on Instantaneous Angular Speed (IAS) Processing and Angular Applications.

- [44] N.C. Xiao, L. Duan, Z. Tang, Surrogate-model-based reliability method for structural systems with dependent truncated random variables, *Proc. Inst. Mech. Eng. O J. Risk Reliab.* 231 (3) (2017) 265–274, <https://doi.org/10.1177/1748006X17698065>.
- [45] Z. Liu, Fast kernel feature ranking using class separability for big data mining, *J. Supercomput.* 72 (8) (2016) 3057–3072, <https://doi.org/10.1007/s11227-015-1481-1>.
- [46] C.W. Hsu, C.J. Lin, A comparison of methods for multiclass support vector machines, *IEEE Trans. Neural Network.* 13 (2) (2002) 415–425, <https://doi.org/10.1109/72.991427>.
- [47] S. Arlot, A. Celisse, A survey of cross-validation procedures for model selection, *Stat. Surv.* 4 (2010) 40–79, <https://doi.org/10.1214/09-SS054>.